Syntheses and Reactions of Vinyl and Phenyl Fragments on Ag(111)

X.-L. Zhou, A. L. Schwaner, and J. M. White*

Contribution from the Department of Chemistry and Biochemistry, University of Texas at Austin, Austin, Texas 78712

Received October 14, 1992

Abstract: Low-energy electron activation of monolayer ethylene and benzene, adsorbed on Ag(111) at 100 K, leads selectively to vinyl and phenyl fragments. An electron impact ionization model, followed by rapid reneutralization and C–H bond cleavage, is proposed. Upon heating, neither fragment undergoes further C–H or C–C bond cleavage; rather, both undergo carbon–carbon coupling to form 1,3-butadiene and biphenyl. When coadsorbed with methyl or ethyl fragments, temperature-programmed desorption yields propene or 1-butene for vinyl, whereas it yields toluene or ethylbenzene for phenyl. Kinetic parameters describing the electron-stimulated fragment synthesis and the subsequent thermal reactions were determined in the presence and absence of atomic iodine.

1. Introduction

The surface chemistry of hydrocarbon fragments, of great importance in catalysis, has been actively studied by the surface science community for many years. The primary focus has been on the structural aspects, kinetic properties, and reaction mechanisms of surface species. Many simple hydrocarbon molecules have been used as models.[1] Previously, thermally driven and photon-driven processes have been used, e.g., halogenated hydrocarbons[2] and other C_xH_y-bearing molecules,[3] to prepare hydrocarbon fragments or intermediates thought to be catalytically important. These approaches are typically limited either because they lead to mixtures of hydrocarbon fragments or because other perturbing coadsorbates, e.g., halogen atoms, are present. There are only a few cases in which a single kind of surface species has been prepared.[4] Recently, we have developed an alternative method, which relies on controlled fluences of low-energy electrons to drive bond-specific nonthermal dissociation.

In the approach we have used, low-energy electrons are incident upon a very weakly held adsorbate, i.e., no rehybridization or strong metal–adsorbate bond. Impact ionization occurs, and the resulting cation is typically reneutralized and quenched to the electronic ground state. However, since the molecule is only weakly coupled to and does not form a chemical bond with the substrate, the quenching rate will be reltively slow, perhaps on the order of picoseconds. Thus, the cation will have a fairly long lifetime, so that an intra-adsorbate C–H bond dissociation is competitive with the quenching. Once dissociation is activated, the resulting fragment will either desorb directly or will form a strong chemical bond with the substrate, e.g., C_2H_5–Ag. This strong bonding makes quenching of subsequent impact ionizations so rapid that further bond dissociation is much less probable. According to this approach, by controlling electron doses and energies, a single kind of hydrocarbon fragment can be synthesized cleanly. Ideally, the hydrocarbon fragments should be more stable thermally than both recombination of H to dihydrogen and desorption of the remaining parent. If so, thermal processing can remove the H and the parent to leave a spectroscopically significant concentration of a single hydrocarbon species. For example, H from electron-induced dissociation of C_2H_4 on Ag(111) bonds less strongly on a metal surface than vinyl fragments. Once prepared, the structures, reactions, and kinetic properties of these surface fragments can be characterized and studied using various surface science tools.

In this article, we report on the thermal reactions of vinyl and phenyl fragments prepared in this way on Ag(111), beginning with adsorbed ethylene and benzene. For benzene (C_6H_6) on Ag(111), the low-energy electron-induced chemistry has been previously reported in detail.[5] For one monolayer, its electron-induced bond-specific dissociation, C–H bond cleavage, to form surface phenyl (C_6H_5) fragments and atomic hydrogen occurs with an electron energy threshold of about 11 eV. The dissociation cross-section increases monotonically with electron energy and lies between 10^{-18} and 10^{-17} cm^2 ($\sim 2 \times 10^{-17}$ cm^2 at 50 eV). At 50 eV, the post-irradiation TPD area of biphenyl, a product of thermally activated coupling of C_6H_5 fragments, increases linearly with the loss of C_6H_6. This was interpreted as a stoichiometric conversion of C_6H_6 to C_6H_5. In this article, we focus on another use of this method: the *kinetics* of the reaction between C_6H_5-(Ph) fragments and CH_3 or C_2H_5 derived from thermal dissociation of CH_3I and C_2H_5I, respectively, to form toluene ($PhCH_3$) and ethylbenzene (PhC_2H_5). Kinetic parameters for these reactions are calculated from fits to transient temperature-programmed reaction profiles.

For C_2H_4 on Ag(111), the qualitative results of electron-induced dissociation at 50 eV have been reported earlier.[6] With instrumental improvements, we found much less acetylene, ethane, and butene in post-irradiation TPD than reported earlier,[6] making it even more difficult to dissociate vinyl. The only other channel detected involves the desorption of minor amounts of molecular C_2H_4. Roughly equal amounts of vinyl are retained and desorbed during electron irradiation. The total cross-section for dissociation and molecular desorption is 5.3×10^{-17} cm^2 at 50 eV; it has a threshold at 10 eV and increases monotonically with electron energy. The reactions of C_2H_3 with CH_3 and C_2H_5 produce propene and 1-butene, respectively.

2. Experimental Section

The experiments were performed in a standard ultrahigh vacuum chamber (UHV) equipped with a UTI-100 quadrupole mass spectrometer (QMS) for temperature-programmed desorption (TPD) and residual gas analysis, a sputtering gun for cleaning the Ag crystal, and a single-pass Auger electron spectrometer (AES). The chamber was pumped with a 360 L/s turbomolecular pump and had a base pressure of 4×10^{-10} Torr.

(1) See, for example: Salmeron, M.; Somorjai, G. A. *J. Phys. Chem.* **1982**, *86*, 341. Greenlief, C. M.; Padloff, P. L.; Zhou, X.-L.; White, J. M. *Surf. Sci.* **1987**, *191*, 93.
(2) Zeara, F. *Acc. Chem. Res.*, submitted for publication.
(3) See, for example: Liu, Z.-M.; Zhou, X.-L.; White, J. M. *Appl. Surf. Sci.* **1991**, *52*, 249.
(4) Ceyer, S. T. *Langmuir* **1990**, *6*, 82.
(5) Zhou, X.-L.; Castro, M. E.; White, J. M. *Surf. Sci.* **1990**, *238*, 215.
(6) Zhou, X.-L.; White, J. M. *J. Phys. Chem.* **1992**, *97*, 7703.

0002-7863/93/1515-4309$04.00/0

The Ag(111) crystal (a disc 2.5 mm thick and 10 mm in diameter) was mounted with two 0.02 in. diameter Ta wires that passed through two 0.02 in. diameter holes drilled in the edge of and parallel to the surface of the crystal. The Ta wires were attached to two 0.094 in. diameter copper rods for resistive heating, typically 3.5 K/s, and for cooling, as low as 90 K, by thermal contact with a liquid nitrogen reservoir. The surface temperature was measured with a chromel–alumel thermocouple spot-welded to a 0.02 in. diameter Ta wire that was pressed into a third hole drilled in the edge of the crystal. The surface was cleaned by Ar^+ sputtering at 90 K followed by annealing at 700 K, and its cleanliness was checked by AES.

Benzene (MCB, 99.5% purity), ethylene (99.5%, Linde), methyl iodide, and ethyl iodide (99.5%, Aldrich) were dosed with the Ag(111) crystal at 90 K through a tubular doser (3 mm i.d.) positioned about 7 mm away from the Ag(111) surface. Prior to the dose, the dissolved gases in benzene, methyl iodide, and ethyl iodide were removed by several freeze–pump–thaw cycles. To prepare for dosing, the crystal was turned away from the doser tube, and the indicated ion gauge pressure was increased $\Delta P = 5 \times 10^{-10}$ Torr. To initiate the dose, the crystal was then turned to face the doser.

Uniform electron irradiation of Ag(111) dosed with one monolayer of C_2H_4 and C_6H_6 was accomplished using electrons emitted from the filament of QMS. The electron energy (5–57 eV) was varied by changing the bias voltage (negative) to the QMS filament with the crystal grounded. The electron flux was estimated by measuring the electron current from the crystal to ground. As discussed in detail earlier,[7] this fails to account for scattered electrons (primary and secondary). Therefore, the reported electron flux is a lower limit and the calculated cross-sections are upper limits. Depending on the bias voltage, the electron current was between 5 and 30 μA. To minimize electron dosing of the sample holder and to avoid electron irradiation during line-of-sight TPD, a stainless steel foil with a ~1.5 cm^2 square hole, covered with a 80% transparent mesh, was placed on, but electrically isolated from, the head of the QMS. During TPD or electron irradiation, the Ag(111) surface was about 5 mm away from the mesh. With this arrangement, only the surface was exposed to electrons. When the foil was floated electrically, there was no current between the sample and ground; when it was grounded, current was detected.

To calculate the thermal activation energy, E_a, and prefactor, θ, for the reaction A(a) + B(a) → C(g), we have adopted an approach described in detail by Parker et al.,[8] which assumes the rate, R, is given by $(\nu^{(n_A+n_B)}/\beta)\theta_A^{n_A}\theta_B^{n_B}\exp(-E_a/kT)$, where θ_A and θ_B are the coverages of A and B, β is the heating rate, and n_A and n_B are reaction orders in A and B, respectively. Our system is rapidly pumped so that R is proportional to the measured desorption intensity of C at time t. The corresponding θ_A and θ_B can be calculated from the remaining integrated partial TPD areas (by integration from time t to infinity). With these experimental quantities in hand, the rate equation can be rearranged to $\ln(R) - n_A \ln(\theta_A) - n_B \ln(\theta_B) = \ln(\nu^{(n_A+n_B)}/\beta) - E_a/RT$, yielding the value of E_a if $\ln(R) - n_A \ln(\theta_A) - n_B \ln(\theta_B)$ versus $1/T$ is linear. When A = B, $R = (\nu^n/\beta)\theta^n \exp(-E_a/kT)$, and a plot of $\ln(R) - n \ln(\theta)$ versus $1/T$ will yield a value of E_a. In either case, we must choose reaction orders and generate the corresponding plots. As described in other work,[8] this method makes use of the full spectrum, which is a distinct advantage.

In passing, we point out that electron-induced dissociation and desorption of adsorbates is a common phenomenon[9] and can be an undesired side effect in TPD if electrons from the mass spectrometer strike the surface. Depending on the adsorbate, the electron-induced dissociation cross-section can be as large as 5×10^{-16} cm^2.[7] Therefore, caution should be taken in TPD, particularly line-of-sight, when surfaces are not protected from electron exposure.

3. Results and Discussion

3.1 Vinyl. A qualitative description of the electron-induced chemistry of C_2H_4 on Ag(111) has been previously reported.[6] While vinyl (C_2H_3) fragments dominated the adsorbed hydrocarbons, the presence of acetylene, ethane, and butene in subsequent temperature-programmed desorption (TPD) suggested that large electron doses led to further C–H bond breaking in vinyl and formation of surface C_2H_2 and C_2H_5 species. In this article, experimental improvements were made which limit electron-driven processes to the sample surface (followed by adsorption on the sample). We find that, even when 80% of the initial C_2H_4 is depleted, H and C_2H_3 are the only detectable electron-induced dissociation products; only butadiene and dihydrogen appear in TPD, and there is no TPD evidence for acetylene, ethane, or butene.

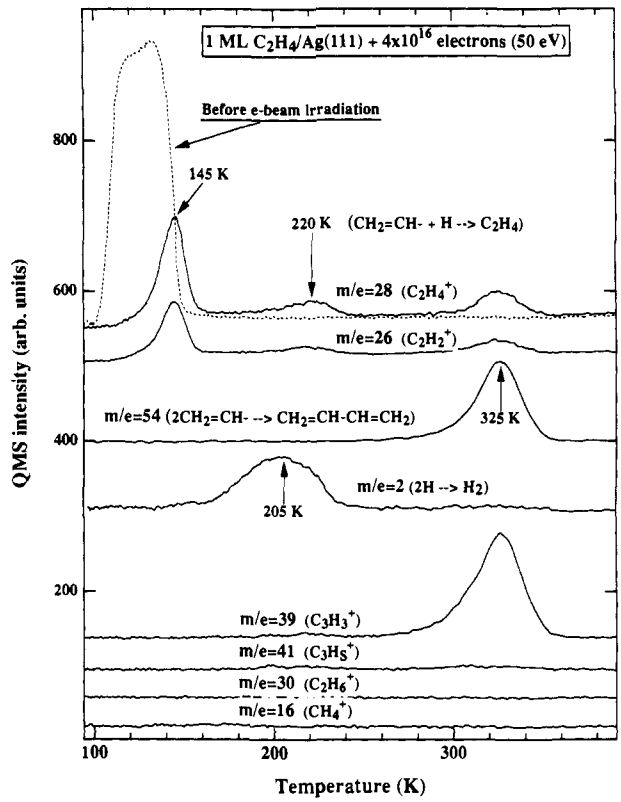

Figure 1. TPD spectra taken after exposing 1 ML of C_2H_4/Ag(111) to 4×10^{16} electrons (50 eV) at 90 K. The broken curve is the C_2H_4 TPD spectrum before electron irradiation. The ramp rate was 3.5 K/s.

3.1.1 Electron-Driven Dissociation and Desorption. Figure 1 shows TPD spectra taken after irradiating 1 ML of C_2H_4/Ag(111) with 4×10^{16} 50-eV electrons (28 μA for 230 s). In the absence of electron irradiation, C_2H_4 is the only desorption species (peak at 130 K), as observed in earlier work.[6] C_2H_4 is weakly π-bonded to Ag(111) and does not rehybridize.[10] After electron irradiation, much less C_2H_4 desorbs, and there are three m/e = 28 peaks: 145, 220, and 325 K. The peak at 145 K is from undissociated, adsorbed C_2H_4, the 220 K peak is from the reaction, H(a) + C_2H_3(a) → C_2H_4(g), and the 325 K peak is from QMS fragmentation of C_4H_6 (see evidence and discussion below). The other TPD products are H_2 (m/e = 2) at 197 K and C_4H_6 (1,3-butadiene, m/e = 54) at 325 K. Neither CH_4 nor C_2H_6 was detected in TPD. Since atomic H on Ag(111) recombines and desorbs with a peak at 197 K,[11] the H_2 observed here is assigned to this process.

The assignment of the m/e = 54 signal to 1,3-butadiene is confirmed by the m/e = 27, 39, 50, and 53 amu signals (not shown except for m/e = 39), which follow the same thermal profile as 54 amu, and the relative intensities measured for C_4H_6. The C_4H_6 desorption is attributed to a recombination-limited process, i.e., $2C_2H_3(a) \rightarrow C_4H_6(g)$, since dosed C_4H_6 on Ag(111) desorbs below 250 K[6] (also see evidence below).

Of the three m/e = 26 ($C_2H_2^+$) peaks, the lower two have the same temperature profiles as the m/e = 28 peaks, and the $(m/e = 26)/(m/e = 28)$ intensity ratio is the same as the QMS

(7) Zhou, X.-L.; Blass, P. M.; Koel, B. E.; White, J. M. *Surf. Sci.* **1992**, *271*, 427.
(8) Parker, D. H.; Jones, M. E.; Koel, B. E. *Surf. Sci.* **1990**, *233*, 65.
(9) Ramsier, R. D.; Yates, J. T., Jr. *Surf. Sci. Rep.* **1991**, *12*, 244.
(10) Felter, T. E.; Weinberg, W. H.; Zhdan, P. A.; Boreskov, G. K. *Surf. Sci.* **1980**, *97*, L313.
(11) Zhou, X.-L.; White, J. M.; Koel, B. E. *Surf. Sci.* **1989**, *218*, 201.

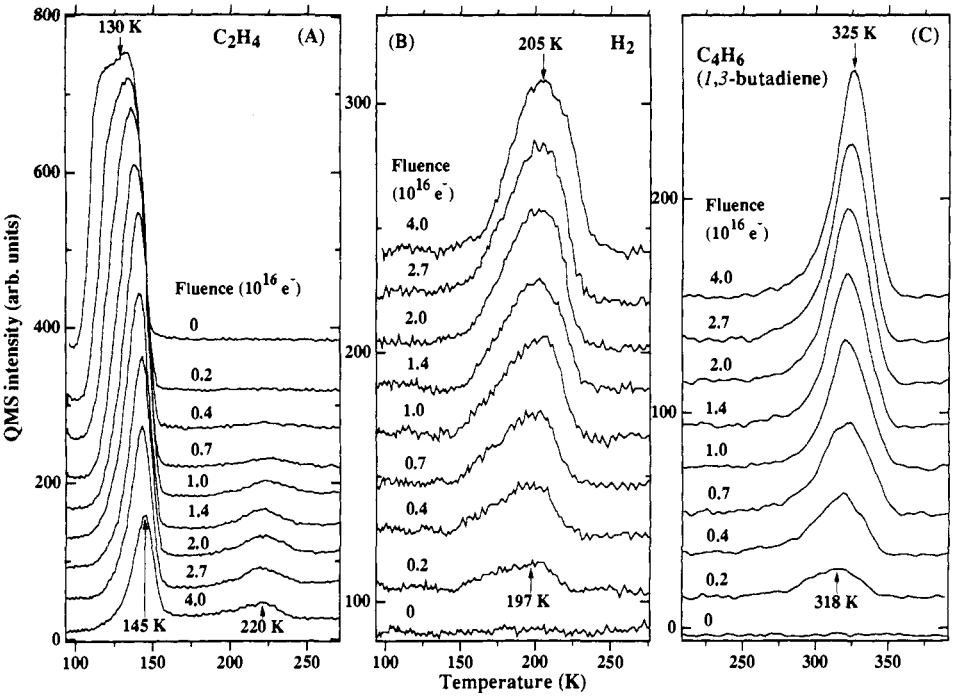

Figure 2. TPD spectra (3.5 K/s) of C_2H_4 (A), H_2 (B), and C_4H_6 (C) taken after exposing 1 ML of C_2H_4/Ag(111) to differing electron fluence (50 eV). The electron fluence is indicated on each curve.

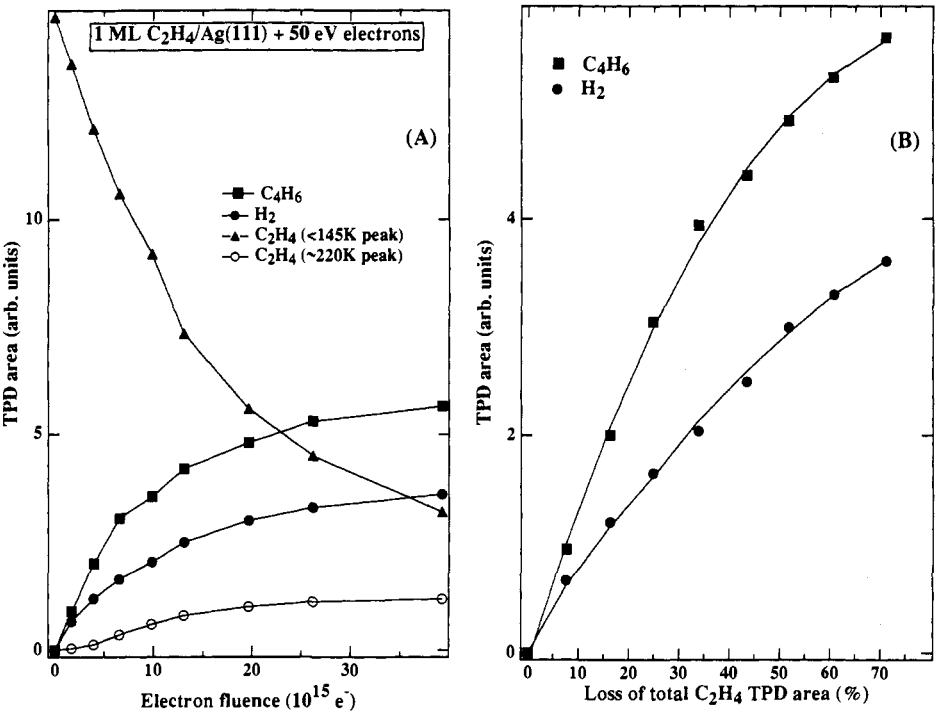

Figure 3. (A) TPD areas of C_2H_4 (<145 K peak), C_2H_4 (~220 K peak), H_2, and C_4H_6 versus electron fluence for 1 ML of C_2H_4/Ag(111). (B) TPD areas of H_2 and C_4H_6 versus loss of total C_2H_4 TPD area.

fragmentation of C_2H_4. The m/e = 26 peak at 325 K is from QMS fragmentation of C_4H_6. We also searched for other C_3 and C_4 hydrocarbons. The TPD traces for m/e = 39 and 41 are shown in Figure 1. There is only one peak, 325 K, for m/e = 39, and it has the same shape and temperature profile as the m/e = 54 peak and the same ratio, $(m/e = 39)/(m/e = 54)$, as dosed C_4H_6. The absence of other peaks for m/e = 39 and 41 demonstrates the absence of other C_3 and C_4 hydrocarbons, since their cracking always produces $C_3H_3^+$ (m/e = 39) and $C_3H_5^+$ (m/e = 41) ions. The absence of C_4 and C_3 hydrocarbons rules out the possibility that C_4H_6 formation involves C_1 and C_3 precursors (e.g., $CH_2 + CHCH{=}CH_2 \rightarrow C_4H_6$). Hydrogenation of C_4 fragments to form C_4H_6 is also ruled out on the basis of the fact that surface H(a) desorbs (as H_2) at temperatures well below where C_4H_6 desorbs. We conclude that C_2H_3 is the only hydrocarbon precursor formed and it leads to C_4H_6. On the basis of AES recorded after TPD, the surface is clean, i.e., no C-containing species remain after C_4H_6 desorbs.

Figure 2 shows, in three panels, how the TPD spectra change with electron fluence (EF) for an initial coverage of one monolayer (ML). Up to 4×10^{16} e, the C_2H_4 intensity decreases, while the peak temperature increases from 130 to 145 K. A new C_2H_4 peak, 220 K, appears at EF = 4×10^{15} e and increases with EF. H_2 intensifies as EF increases, but its peak temperature increases

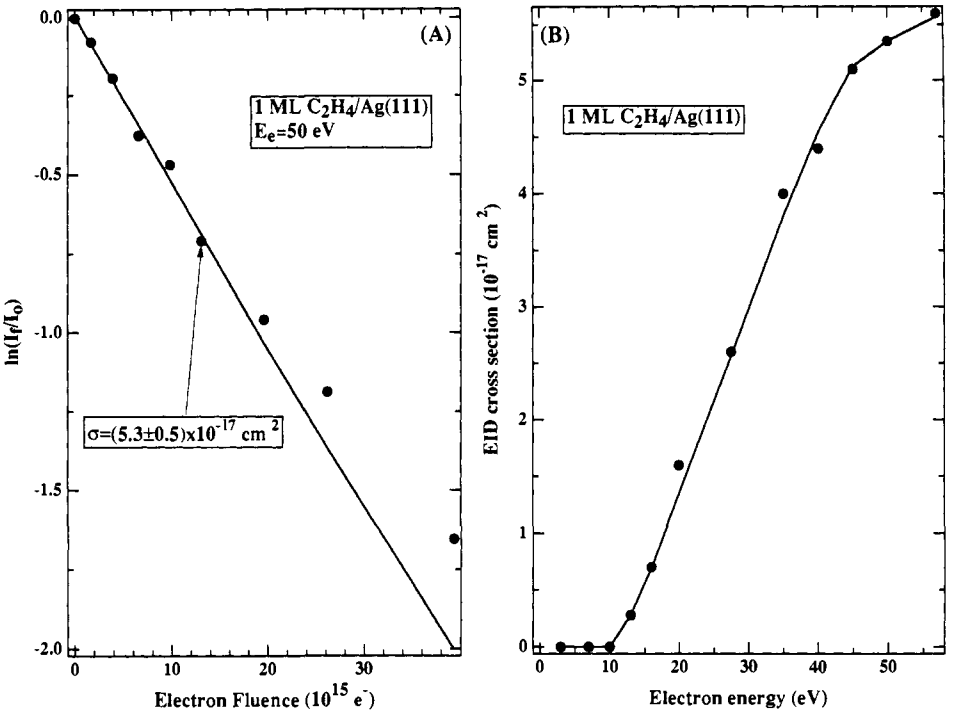

Figure 4. (A) Semilogarithmic plot of ln (I_f/I_o) versus electron fluence for 1 ML of C_2H_4/Ag(111) exposed to 50-eV electrons, where I_o and I_f are TPD areas of C_2H_4 desorbing below 145 K before and after electron irradiation, respectively. (B) Cross-section of electron-induced processes for 1 ML of C_2H_4/Ag(111) versus electron energy.

only slightly (from 197 to 205 K). C_4H_6 also intensifies and its peak temperature shifts upward slightly (from 318 to 325 K).

With an initial coverage of 1 ML, the total amounts desorbed (peak areas) are summarized in Figure 3A. The TPD areas of H_2 and C_4H_6 versus the loss of total C_2H_4 TPD area (200 K peak plus the lower T peak) are plotted in Figure 3B. H_2 and C_4H_6 increase monotonically with the loss of C_2H_4 area, reflecting conversion of π-bonded C_2H_4(a) to H(a) and C_2H_3(a). However, the correlation is not linear as is expected if electron exposure involves only the formation of adsorbed vinyl and atomic hydrogen. As will be shown later, the desorption of C_2H_4 and C_2H_3 occurs during electron irradiation.

From Figure 4A, we estimate the total cross-section describing all electron-induced processes that remove C_2H_4. Here I_o and I_f are TPD areas, before and after electron irradiation of C_2H_4 desorbing between 105 and 160 K. Because the desorption of C_2H_4 at 220 K is also a result of electron irradiation, it is not included in I_f. Figure 4A shows the plot of ln (I_f/I_o) versus EF. For 50-eV electrons, this semilog plot is linear for EF $< 2 \times 10^{16}$ e and the slope yields a quite large cross-section of $(5.3 \pm 0.5) \times 10^{-17}$ cm^2. The trend toward a lower slope for high EFs is attributed to the accumulation of electron-induced dissociation products, H(a) and C_2H_3(a), which lowers the probability of electron-induced processes. As discussed in section 2, the cross-section determined in this way is an upper limit because scattered electrons are not accounted for in EF.

Cross-sections calculated in this way show an electron energy dependence (Figure 4B). There is a threshold near 10 eV, above which the cross-section increases monotonically: rapidly to 40 eV and then slowly. The gas-phase ionization potential of C_2H_4 is ~10 eV; thus, we propose that the electron-induced chemistry observed here is initiated by electron impact ionization.

As noted above, there is desorption during the electron dose. With an initial coverage of 1 ML, Figure 5 shows isothermal (90 K) spectra of m/e = 25–28 ($C_2H_x^+$, x = 1–4), measured during electron irradiation. We also searched for H_2, CH_4, C_2H_6, and $C_{\geq 3}$ hydrocarbons during electron irradiation, but they were not observed. When the electron flux is initiated, the $C_2H_x^+$ (x = 1–4) intensities rise promptly to a maximum and then decay.

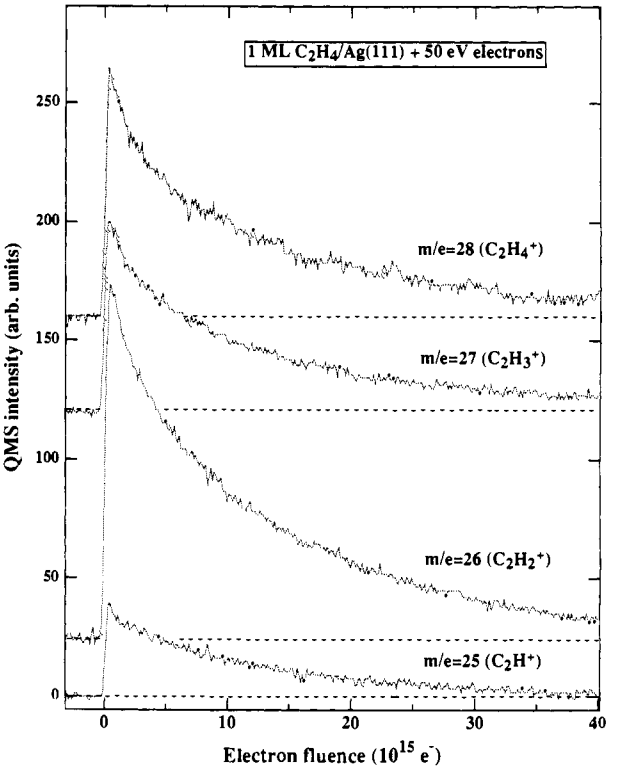

Figure 5. Isothermal spectra of m/e = 25 (C_2H^+), 26 ($C_2H_2^+$), 27 ($C_2H_3^+$), and 28 ($C_2H_4^+$) signals taken during electron (50 eV) irradiation of 1 ML of C_2H_4/Ag(111) at 90 K.

Interestingly, the relative intensities (C_2H^+):($C_2H_2^+$):($C_2H_3^+$):($C_2H_4^+$) of 0.23:1.44:0.78:1 are different from those (0.15:0.55:0.58:1) found for the fragmentation of C_2H_4 in our QMS. This is strong evidence that other species in addition to C_2H_4 are desorbing during electron irradiation. One possibility is acetylene, since $C_2H_2^+$ is the strongest signal in Figure 5. However, the absence of C_2H_2 in post-irradiation TPD suggests that this is unlikely. Rather, we propose that a significant fraction of the

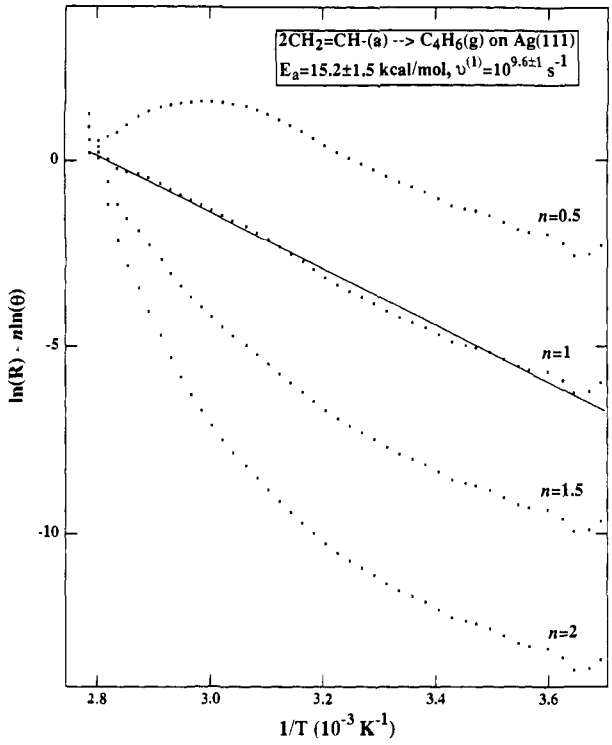

Figure 6. Kinetic analysis of a vinyl coupling reaction. $\ln(R) - n\ln(\theta)$ versus $1/T$ for the $2CH_2{=}CH(a) \rightarrow C_4H_6(g)$ reaction on Ag(111) (data from Figure 1), where R is the reaction rate (which is proportional to the TPD intensity of C_4H_6), n the reaction order, and θ the $CH_2{=}CH$ coverage (which is proportional to TPD area).

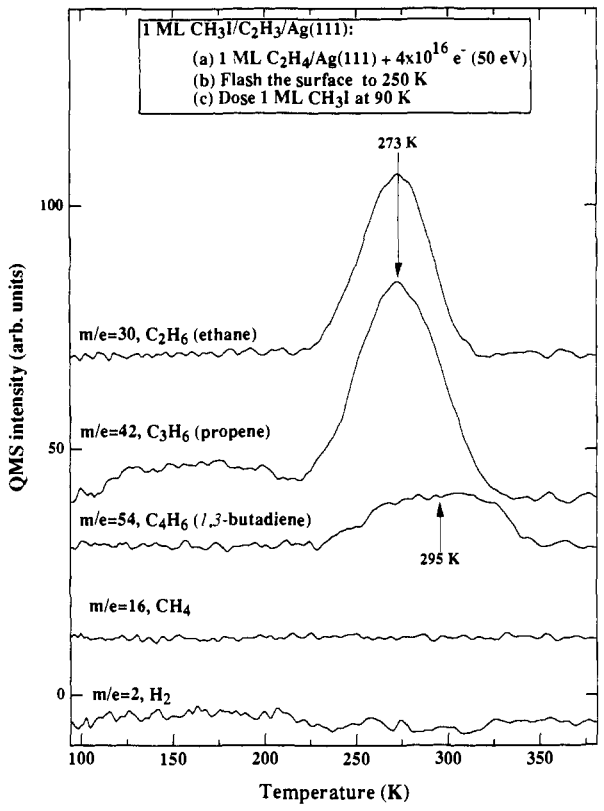

Figure 7. TPD spectra taken after dosing ~1 ML of CH_3I on C_2H_3/Ag(111) at 90 K. The C_2H_3/Ag(111) surface was prepared by exposing 1 ML of C_2H_4/Ag(111) to 4×10^{16} electrons (50 eV) at 90 K followed by flashing to 250 K.

C_2H_3 fragments desorb. While we do not know the cracking pattern of C_2H_3, its fragmentation to $C_2H_2^+$ is not unexpected. Comparing intensities integrated over time, we conclude that no more than 10% of the initial C_2H_4 (1 ML) is molecularly desorbed when 80% of the initial C_2H_4 is depleted. Therefore, 0.7 ML C_2H_4 dissociates for an irradiation with 4×10^{16} e (50 eV). Clearly, electron-induced parent desorption is a minor process; the formation of vinyl and atomic hydrogen dominate. For an EF of 4×10^{16} e at 50 eV, the 1,3-butadiene TPD area is 30% of the area measured for monolayer 1,3-butadiene (directly dosed). This is a spectroscopically significant amount even though the absolute coverage in terms of butadiene molecules per surface Ag atom is unknown.

3.1.2 Thermal Vinyl Recombination. Having discussed the electron-induced dissociation and desorption of C_2H_4 on Ag(111), we now turn to thermal reactions of C_2H_3 fragments. According to Figure 1, heating to 250 K after the electron dose will leave a surface free of adsorbed H and C_2H_4 and, as proposed above, covered with vinyl (C_2H_3). These recombine to form 1,3-butadiene at 325 K. However, the $2C_2H_3(a) \rightarrow C_4H_6(g)$ reaction does not exhibit typical second-order kinetics (i.e., the peak temperature should decrease, but it increases, with increasing C_2H_3 coverage). Figure 6 shows the plots of $\ln(R) - n\ln(\theta)$ versus $1/T$ (see section 2) for $n = 0.5, 1, 1.5$, and 2 over the entire desorption temperature range. It is obvious from Figure 6 that only the plot for $n = 1$ is linear, indicating that the reaction is first-order. From the slope, $E_a = 15.2 \pm 1.5$ kcal/mol is derived. The derivative of the rate equation (see section 2) with respect to temperature is zero at desorption peak temperature, T_p. After the derivative is taken, the prefactor can be calculated from $\nu^{(1)} = \beta(E_a/kT_p^2)\exp(E_a/kT_p)$ for a first-order reaction. Substitution of 15.2 ± 1.5 kcal/mol and 325 K for E_a and T_p, respectively, yields $\nu^{(1)} = 10^{9.6\pm1}$ s^{-1}. The first-order behavior of this reaction is rather surprising and the reason is not clear.

3.1.3 Vinyl Plus Methyl. We have also studied the reactions of C_2H_3 with CH_3 and C_2H_5 fragments derived from thermal dissociation of CH_3I and C_2H_5I, respectively. These adsorbed iodides dissociate between 140 and 200 K to produce CH_3,[12] C_2H_5,[13] and atomic iodine. Vinyl was prepared first by exposing 1 ML of C_2H_4/Ag(111) to 4×10^{16} 50-eV electrons at 90 K, followed by flashing the surface to 250 K to desorb hydrogen and undissociated C_2H_4. Approximately 1 ML of CH_3I or C_2H_5I was dosed after cooling to 90 K.

Figure 7 shows the TPD spectra for CH_3I/C_2H_3/Ag(111). Among the CH-containing products, ethane (C_2H_6), propene (C_3H_6), and butadiene (C_4H_6) desorbed; H_2, CH_4, and other hydrocarbons were not found. CH_3I (205 K) and atomic iodine (845 K) (not shown) were the only other desorbing species detected. Propene dominates the products and peaks at 273 K. It is attributed to a reaction-limited process, i.e., $CH_3(a) + C_2H_3(a) \rightarrow C_3H_6(g)$, because dosed C_3H_6 desorbs at a much lower temperature (165 K). The formation of C_3H_6 is, again, strong evidence that C_2H_3 fragments are produced from electron-induced dissociation of C_2H_4/Ag(111). Ethane formation, also peaking at 273 K, is attributed to carbon–carbon coupling between CH_3 fragments, i.e., $2CH_3(a) \rightarrow C_2H_6(g)$. Butadiene, attributed to the coupling of vinyl fragments, desorbs at a lower temperature (~290 K) than C_2H_3 on clean Ag(111) (325 K), indicating a significant effect of surface iodine. Since both ethane and propene formation involve methyl fragments, and since both peak at the same temperature, we suggest that the diffusion of methyl groups controls the formation rates. Consistent with this notion, butadiene formation, which requires vinyl motion, occurs at a higher temperature. Comparing the propene area in Figure 7 with that measured for its monolayer (ML) saturation (directly dosed C_3H_6, not shown), we calculate that the amount desorbing in Figure 7 corresponds to 0.2 ML. The TPD area of C_4H_6 in Figure 7 is 48% of that measured in the absence of CH_3I (0.18

(12) Zhou, X.-L.; Solymosi, F.; Blass, P. M.; Cannon, K. C.; White, J. M. *Surf. Sci.* **1989**, *219*, 294.
(13) Zhou, X.-L.; White, J. M. *Catal. Lett.* **1989**, *2*, 375.

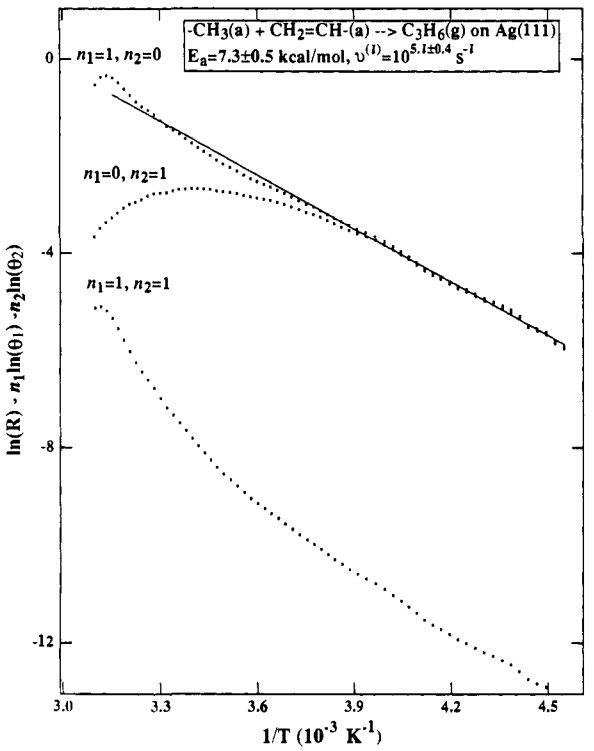

Figure 8. Kinetic analysis of a coupling reaction of methyl and vinyl, i.e., $CH_3(a) + CH_2{=}CH(a) \rightarrow C_3H_6(g)$, on I/Ag(111) (data from Figure 7). n_1 and n_2 are reaction orders in CH_3 and $CH_2{=}CH$, respectively, and θ_1 and θ_2 are coverages of CH_3 and $CH_2{=}CH$, respectively. See the text for details of this plot.

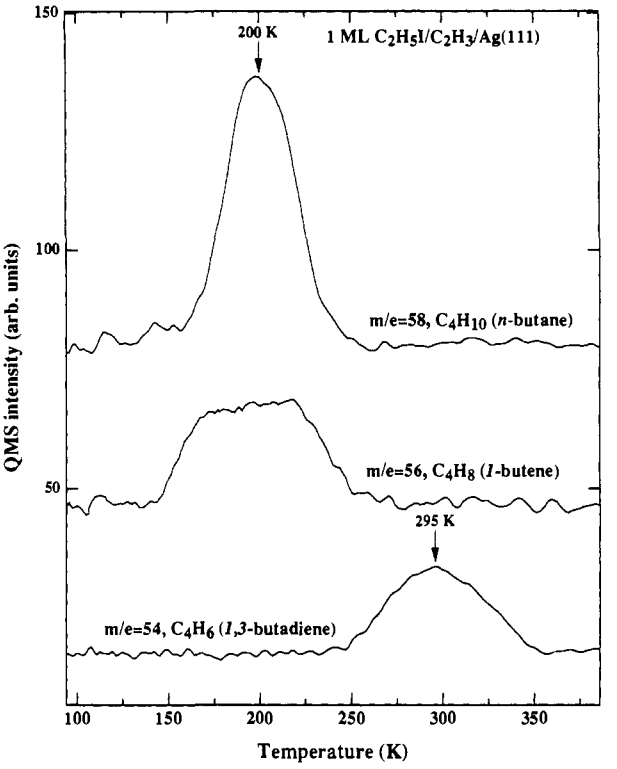

Figure 9. TPD spectra taken after dosing ~1 ML of C_2H_5I on C_2H_3/Ag(111) at 90 K. The C_2H_3/Ag(111) surface was prepared by exposing 1 ML of C_2H_4/Ag(111) to 4×10^{16} electrons (50 eV) at 90 K followed by flashing to 250 K.

ML equiv of vinyl). Thus, we prepared 0.38 ML of C_2H_3 fragments by this electron beam method, which was certainly spectroscopically significant and encouraged us to begin vibrational characterization. For an irradiation with 4×10^{16} e (50 eV), 0.7 ML of C_2H_4 dissociated to form vinyl and hydrogen, indicating that roughly one-half of the vinyl fragments produced from C_2H_4 are retained at the surface if we assume the same surface density for 1 ML of C_2H_4 and C_3H_6.

Turning to the reaction kinetics of $CH_3(a) + C_2H_3(a) \rightarrow C_3H_6(g)$, we plotted $\ln(R) - n_1 \ln(\theta_1) - n_2 \ln(\theta_2)$ versus $1/T$ following the procedure outlined in section 2, where θ_1 and θ_2 are the coverages of CH_3 and C_2H_3, and n_1 and n_2 are the reaction orders in CH_3 and C_2H_3, respectively. R is proportional to the intensity of ion signals monitoring C_3H_6, and relative values for θ_1 and θ_2 can be numerically calculated from the TPD spectra. To achieve this, we converted the TPD areas of C_2H_6 and C_4H_6 to equivalent C_3H_6 areas. Thus, θ_1 is proportional to the TPD area of $[(C_2H_6) + (C_3H_6)/2]$ and θ_2 to the TPD area of $[(C_4H_6) + (C_3H_6)/2]$. A linear plot, over a reasonable temperature (and concentration) range, is found for $\ln(R) - \ln(\theta_1)$ versus $1/T$ (Figure 8). This indicates that the reaction is first-order in CH_3 and zero-order in C_2H_3, consistent with the notion that the reaction is activated by CH_3 diffusion. From Figure 8, $E_a = 7.3 \pm 0.5$ kcal/mol and $\nu^{(1)} = 10^{5.1 \pm 0.4}$ s^{-1}.

3.1.4 Vinyl Plus Ethyl. Figure 9 shows the TPD spectra for 1 ML of C_2H_5I/C_2H_3/Ag(111). In this case, *n*-butane (C_4H_{10}), *l*-butene (C_4H_8), and butadiene (C_4H_6) were the only reaction products found in TPD. Molecular C_2H_5I desorption is negligible; there is only a tiny peak at 160 K. Surface iodine desorbs atomically at 835 K. The coupling of C_2H_5 fragments to form C_4H_{10} occurs between 150 and 250 K with a peak at 200 K, in agreement with our earlier work.[13] The coupling reaction of ethyl and vinyl to form butene ($C_2H_5 + C_2H_3 \rightarrow C_4H_8$) also occurs in this temperature regime. As above, we supposed that C_2H_5 diffusion controls the rates. Since the C_4H_8 desorption peak is not well-defined, possibly indicating more than one reaction, we did not attempt to determine an activation energy and prefactor. Following the procedure outlined in section 2, kinetic analysis (not shown) of the C_4H_{10} spectrum indicates that butane formation is first-order in the concentration of ethyl fragments, with $E_a = 4.5 \pm 0.4$ kcal/mol and $\nu^{(1)} = 10^{4.8 \pm 0.5}$ s^{-1}. From the nature of the TPD spectra, the kinetic parameters for the butene formation will probably be similar.

In Figure 9, C_4H_6 desorption peaks at 295 K, which is lower than C_2H_3 on clean Ag(111) (i.e., containing no coadsorbed iodine). Kinetic analysis indicates a first-order reaction in vinyl, but with very different kinetic parameters than in the absence of iodine, i.e., $E_a = 6.3 \pm 0.6$ kcal/mol and $\nu^{(1)} = 10^{3.9 \pm 0.4}$ s^{-1} compared to $E_a = 15.2 \pm 1.5$ kcal/mol and $\nu^{(1)} = 10^{9.6 \pm 1}$ s^{-1} on an iodine-free surface. Thus, coadsorbed iodine does not alter the reaction pathway, but it has a dramatic influence on the kinetic parameters; as is often observed, when the activation energy is lowered, the prefactor tends to compensate.

3.1.5 Vinyl Plus Water. On Ag(111), water does not dissociate, and it desorbs well below the temperature where our results suggest that vinyl will become thermally activated. Thus, to give further insight into the activity of vinyl fragments, we briefly examined the coadsorption of H_2O with C_2H_3 on Ag(111). In TPD, there was no evidence of a reaction; H_2O desorbed at 165 K and C_4H_6 at 325 K. This is entirely consistent with our model; vinyl fragments do not become active until after all of the water desorbs. We intend to examine OH (electron-induced decomposition of water) coadsorbed with C_2H_3, since acetaldehyde (CH_3CHO) formation is expected.

3.2 Phenyl. We now turn to the reactions of phenyl fragments on Ag(111). We will focus only on the thermal reactions of C_6H_5 with CH_3 and C_2H_5 fragments, because detailed results of low-energy (5–50 eV) electron-induced chemistry of C_6H_6 on Ag(111) have been reported earlier.[5]

3.2.1 Phenyl Recombination. Figure 10 shows the TPD spectra taken before and after exposure of 1 ML of C_6H_6/Ag(111) to 6×10^{16} 50-eV electrons. Before electron exposure, C_6H_6 desorbs

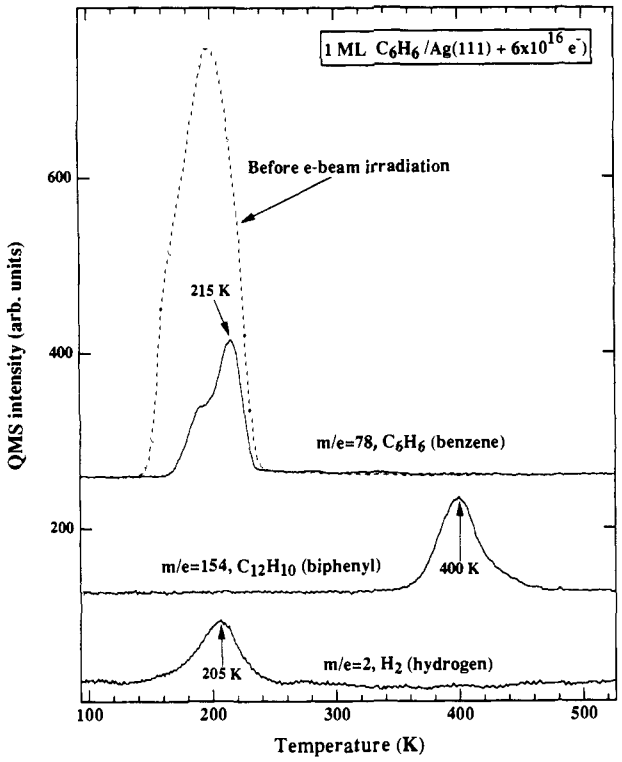

Figure 10. TPD spectra (3.5 K/s) taken after exposing 1 ML of benzene/Ag(111) to 6×10^{16} electrons (50 eV) at 90 K. The broken curve is the C_6H_6 TPD spectrum before electron irradiation.

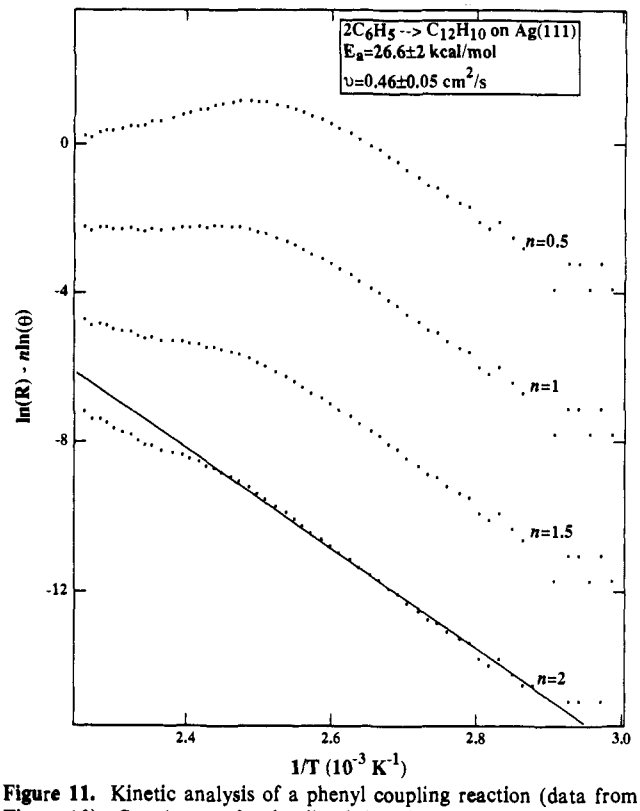

Figure 11. Kinetic analysis of a phenyl coupling reaction (data from Figure 10). See the text for details of this plot.

as a relatively broad peak at 200 K. After exposure, H_2, C_6H_6, and $C_{12}H_{10}$ (biphenyl) were the only species desorbing, in agreement with our earlier work.[5] During electron irradiation, we searched for desorbing species by mass spectrometry, e.g., H_2, C_6H_6, C_6H_5, and $C_{12}H_{10}$, but found none. As expected, much less (75% less) benzene desorbs. In addition, the hint of a shoulder before the electron dose is now easily recognized. Thermally activated recombination of C_6H_5 fragments produces $C_{12}H_{10}$, and H_2 is the result of recombination of H atoms bound to Ag.[5]

Kinetic analysis of the biphenyl formation reaction, $2C_6H_5$-(a) $\rightarrow C_{12}H_{10}$(g), is illustrated in Figure 11. Although for every n there are regions over which the plot is linear, $n = 2$ clearly gives the best fit, indicating that C_6H_5 coupling to form $C_{12}H_{10}$-(g) is a second-order reaction. Unlike the first-order coupling of vinyl to form butadiene, coupling of phenyl fragments to form biphenyl appears to require lateral motion (diffusion) of both fragments. From the slope, $E_a = 26.6 \pm 2$ kcal/mol. In order to obtain the prefactor, we assume that the electron-induced conversion of adsorbed benzene to adsorbed phenyl is stoichiometric, supported by the facts that no hydrocarbon species desorb during electron irradiation and that the TPD area of $C_{12}H_{10}$ increases linearly with the loss of C_6H_6.[5] With one-to-one stoichiometry and 1 ML C_6H_6 coverage on Ag(111) of 1.2×10^{14} molecules/cm^2,[5] we calculate a phenyl (C_6H_5) coverage, θ, of 8.6×10^{13} molecules/cm^2. For a second-order rate coefficient, $\nu^{(2)} = \beta(E_a/kT_p^2)\exp(E_a/kT_p)/2\theta$, where T_p is the desorption peak temperature. We calculate $\nu^{(2)} = 10^{-0.2\pm1}$ cm^2/s.

3.2.2 Phenyl Plus Methyl and Ethyl. We now turn to reactions of C_6H_5 with CH_3 and C_2H_5 fragments. The phenyl-covered surface was prepared by exposing 1 ML of C_6H_6/Ag(111) to 6×10^{16} 50-eV electrons at 90 K, flashing to 300 K to desorb undissociated C_6H_6 and H_2, and recooling to 90 K. Then approximately 1 ML of CH_3I or C_2H_5I was dosed, and the TPD spectra were measured. For the CH_3I case (Figure 12), C_2H_6 (285 K), $C_{12}H_{10}$ (395 K), toluene (245 and 295 K), molecular CH_3I (198 K, not shown), and atomic iodine (850 K, not shown) were observed. The formation of toluene ($PhCH_3$), ascribed to the coupling of CH_3 and C_6H_5, is confirming evidence that C_6H_5 fragments are synthesized by electron-driven dissociation of C_6H_6.

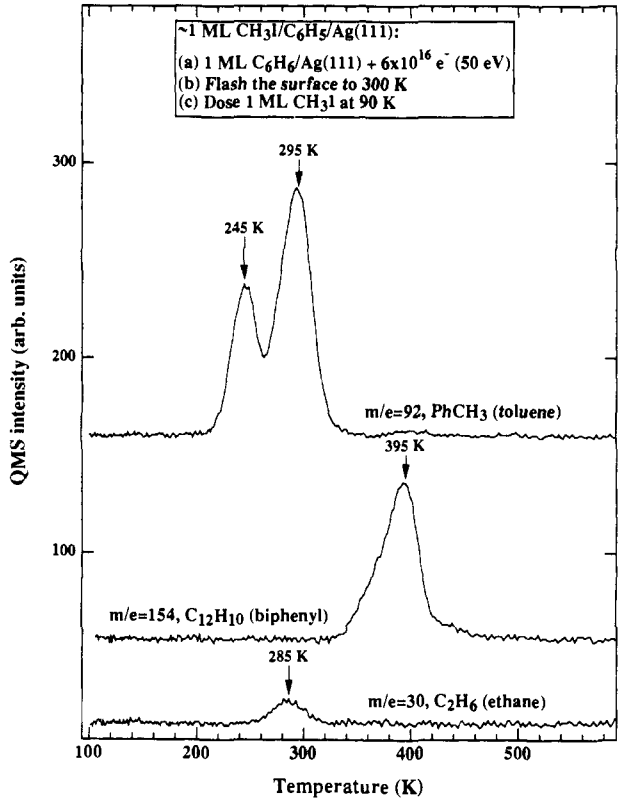

Figure 12. TPD spectra (3.5 K/s) taken after dosing ~1 ML of CH_3I on C_6H_5/Ag(111) at 90 K. The C_6H_5/Ag(111) surface was prepared by exposing 1 ML of benzene/Ag(111) to 6×10^{16} electrons (50 eV) at 90 K followed by flashing to 300 K.

There are two well-resolved toluene TPD peaks. To provide insight into their origins, we dosed toluene and measured the

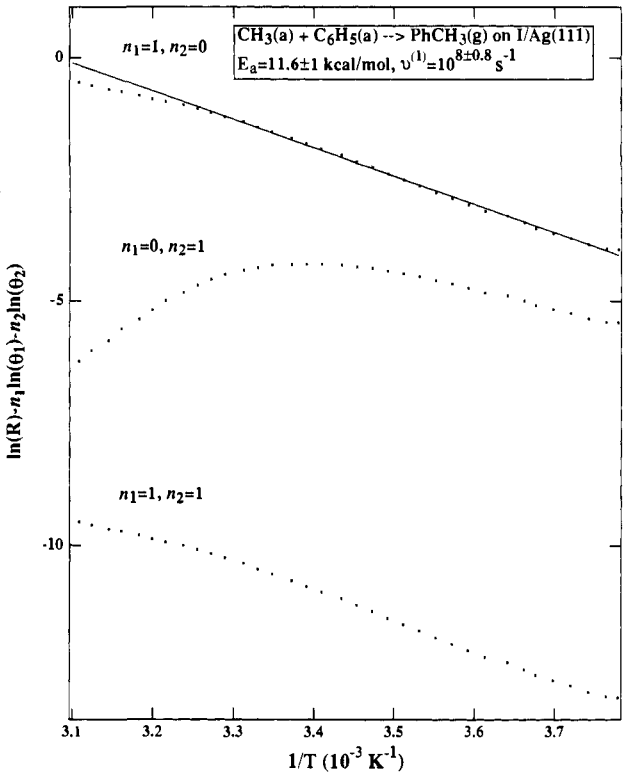

Figure 13. Kinetic analysis of the coupling of methyl with phenyl. n_1 and n_2 are reaction orders in CH_3 and C_6H_5, respectively, and θ_1 and θ_2 are coverages of CH_3 and C_6H_5, respectively. See the text for details of this plot.

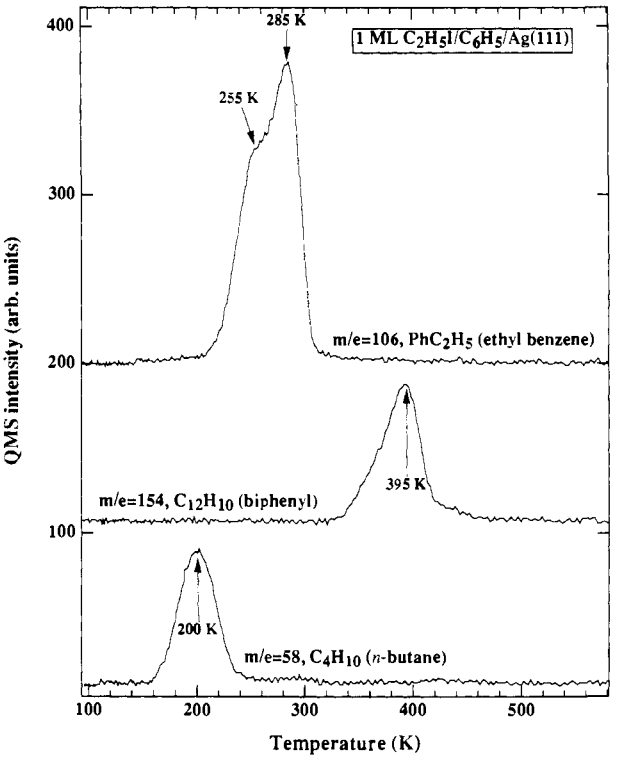

Figure 14. TPD spectra (3.5 K/s) taken after dosing ~1 ML of C_2H_5I on C_6H_5/Ag(111) at 90 K. The C_6H_5/Ag(111) surface was prepared by exposing 1 ML of benzene/Ag(111) to 6×10^{16} electrons (50 eV) at 90 K followed by flashing to 300 K.

TPD spectra. As expected, there is no decomposition. The peak temperature (~240 K) shifts downward slightly with increasing coverage. With submonolayer amounts of I(a), the peak temperature increases by 10–15 K. These desorption temperatures are lower than those observed when phenyl and methyl couple, and they show that the rate-determining step in $CH_3(a) + C_6H_5(a) \rightarrow PhCH_3(g)$, which peaks at 295 K, is the coupling reaction, not the desorption of toluene. We cannot determine the rate-limiting step in toluene evolution at 245 K in Figure 12. Xi and Bent[14] observed a $PhCH_3$ peak on Cu(111) at 385 K for coupling methyl and phenyl and another toluene peak under some conditions at 240 K, which they attribute to a reaction between molecular CH_3I and C_6H_5 fragments. A similar reaction may be taking place on Ag; if so, it must occur below 240 K, since CH_3I desorbs at a lower temperature (198 K).

The toluene peak area in Figure 12 is 17% of that found when toluene is dosed to monolayer coverage (defined as 1 ML), while the biphenyl area is 75% of that found in the absence of coadsorbed CH_3I. Thus, we calculate that the C_6H_5 coverage, prepared by electron irradiation, corresponds to 0.7 ML of $PhCH_3$, which is very close to the amount of C_6H_6 lost (0.75% of the initial coverage). If the absolute coverages of the first layer C_6H_6 and $PhCH_3$ are the same, then the electron-driven conversion of C_6H_6-(a) to C_6H_5(a) is nearly stoichiometric.

Regarding the kinetics of $CH_3(a) + C_6H_5(a) \rightarrow PhCH_3(g)$, Figure 13 shows three fits related to the 295 K TPD peak. While the plot for $n_1 = 0$, $n_2 = 1$ is nonlinear, the plots for both $n_1 = 1$, $n_2 = 0$ and $n_1 = 1$, $n_2 = 1$ are linear and have nearly the same slope, although they are offset by 9.2 (arbitrary unit). Here, n_1 and n_2 are reaction orders in CH_3(a) and C_6H_5(a), respectively. We note that, for Figure 12, the relative coverage of C_6H_5 is much higher than that of CH_3 (θ_2:θ_1 = 1:0.21). Therefore, ln (θ_2) is roughly constant, resulting in nearly the same slope, and there is a large offset. In either case, the reaction is first-order in CH_3< and the slope yields $E_a = 11.6 \pm 1$ kcal/mol. If we assume that the reaction is pseudo-first-order, the pre-exponential factor is $\nu^{(1)} = 10^{8\pm0.8}$ s^{-1}. For comparison, the coupling of C_6H_5 and CH_3 groups to form toluene on Cu(111) in the presence of coadsorbed iodine occurs at 385 K.[14] By assuming a pseudo-first-order pre-exponential factor of 10^{13} s^{-1}, Xi and Bent[14] calculated an activation energy of 24 kcal/mol for the toluene formation from C_6H_5 and CH_3 on Cu(111).

Kinetic analysis of the $C_{12}H_{10}$ peak in Figure 12 gives $E_a = 22.2 \pm 2$ kcal/mol and $\nu^{(2)} = 10^{-2.5\pm1}$ cm^2/(molecule·s), i.e., second-order gives the best fit. However, the activation energy is lower than on clean Ag (26.6 kcal/mol). Clearly, coadsorbed atomic iodine tends to lower the activation energies for both vinyl and phenyl couplings on Ag(111). In comparable work, Xi and Bent[14] used iodobenzene as a precursor for the preparation of C_6H_5 fragments on Cu(111). They found that coupling to form biphenyl, in the presence of coadsorbed iodine, occurs at 350–385 K. Assuming a standard pseudo-first-order preexponential factor of 10^{13} s^{-1} for the C_6H_5 coupling reaction, they obtained an activation energy of 23 kcal/mol. While the justification of their assumption is necessary, this value is essentially the same as that for the coupling on iodine-coveraged Ag(111) (22.2 ± 2 kcal/mol), but is lower than the 26.6 ± 2 kcal/mol for C_6H_5 coupling on clean Ag(111). This suggests that the energy barrier for the C_6H_5 coupling reaction on both Cu(111) and Ag(111) in the presence of coadsorbed iodine is the same.

Switching from methyl to ethyl, we show in Figure 14 the TPD spectra for 1 ML of C_2H_5I/C_6H_5/Ag(111). In addition to a peak at 835 K for atomic iodine and a tiny peak for C_2H_5I at 170 K, ethylbenzene (PhC_2H_5), C_4H_{10}, and $C_{12}H_{10}$ were the only species found in TPD. Ethylbenzene desorption peaks at 285 K and has a definite shoulder at 255 K; butane peaks at 200 K, and biphenyl at 395 K. Because C_2H_5 coupling to form C_4H_{10}, which promptly desorbs, occurs at a much lower temperature than the desorption of PhC_2H_5, the latter must be formed at or below 200 K, i.e., the rate-determining step in the evolution of PhC_2H_5 between 255 and 285 K is PhC_2H_5 desorption, not the coupling

(14) Xi, M.; Bent, B. E. *Surf. Sci.*, in press; *Science*, in press.

reaction. This reasoning is supported by the fact that PhC_2H_5 dosed to monolayer coverage desorbs with a peak at 250 K in the absence of, and at 275 K in the presence of, atomic I. With regard to kinetics, we suppose, but cannot prove, that $C_2H_5(a) + C_6H_5(a) \rightarrow PhC_2H_5(a)$, like ethyl coupling, is activated by C_2H_5 diffusion, and, thus, has the same activation energy, i.e., $E_a = 4.4$ kcal/mol.

On Cu(111), Xi and Bent studied the coadsorption and reaction of C_2H_5I with C_6H_5 (and atomic iodine) formed by 18-eV electron-induced dissociation of adsorbed C_6H_5I at 120 K. They observed only one PhC_2H_5 desorption peak at 160 K and attributed it to reaction between C_6H_5 and C_2H_5I, a reaction which may make a minor contribution on Ag(111). The absence of a high-temperature PhC_2H_5 peak involving C_6H_5 and C_2H_5 coupling was attributed to β-elimination of ethyl to form ethylene at 250 K. Because C_2H_5 groups do not undergo β-elimination on Ag(111),[13] the coupling between C_6H_5 and C_2H_5 is expected.

4. Commentary

The results presented in section 3 provide evidence that low-energy electron impact activation of adsorbed ethylene and benzene can lead, with excellent selectivity, to spectroscopically significant amounts of vinyl and phenyl fragments on Ag(111). We believe that a variety of catalytically important fragments can be synthesized on a variety of metal surfaces with this method by selecting an appropriate precursor molecule and adjusting the experimental conditions, e.g., surface temperature, electron energy, and flux. Once prepared, the surface structures and transient reactions of these species can be characterized. In our laboratory, vibrational characterization of vinyl and phenyl fragments on Ag(111) prepared by this method is currently in progress.

5. Summary and Conclusions

(1) By irradiation with controlled fluences of low-energy ($\leq$57 eV) electrons, spectroscopically significant amounts of vinyl and phenyl fragments can be synthesized on Ag(111) from adsorbed monolayers of ethylene and benzene, respectively. This method may be generalized for selectively preparing a variety of catalytically important fragments or intermediates on various metal surfaces.

(2) On Ag(111), neither vinyl nor phenyl fragments thermally decompose; rather, they undergo carbon–carbon coupling reactions to form 1,3-butadiene and biphenyl, respectively. The 1,3-butadiene formation, from vinyl fragments at 325 K, is a first-order reaction with $E_a = 15.2 \pm 1.5$ kcal/mol and $\nu^{(1)} = 10^{9.6\pm1}$ s^{-1}. Biphenyl formation occurs at 400 K and is a second-order reaction with $E_a = 26.2 \pm 2$ kcal/mol and $\nu^{(2)} = 10^{-0.2\pm1}$ cm^2/(molecule·s). Coadsorbed atomic iodine does not alter the reaction pathways, but does lower the activation energy for the coupling reactions: $E_a = 6.3 \pm 0.6$ kcal/mol for vinyl coupling and $E_a = 22.2 \pm 2$ kcal/mol for phenyl coupling.

(3) Vinyl reacts with CH_3 and C_2H_5 fragments on Ag(111), derived from thermal dissociation of CH_3I and C_2H_5I, respectively, to form propene and 1-butene. Propene formation occurs at 273 K and is overall a first-order reaction (first-order in CH_3 and zero-order in vinyl) with $E_a = 7.5 \pm 0.5$ kcal/mol and $\nu^{(1)} = 10^{5.1\pm0.4}$ s^{-1}. The 1-butene forms at $\sim$200 K and probably has the same activation energy (4.4 ± 0.4 kcal/mol) as C_2H_5 coupling to form butane.

(4) Phenyl reacts with CH_3 and C_2H_5 fragments on Ag(111) to form toluene and ethylbenzene, respectively. Toluene forms by coupling methyl and phenyl fragments at 295 K. The process is first-order in CH_3 with $E_a = 11.6 \pm 1$ kcal/mol and a prefactor of $10^{8\pm0.8}$ s^{-1}. Some phenyl may also react with CH_3I at or below 200 K to form toluene that desorbs at 245 K. Ethylbenzene is formed at or below 200 K and, with desorption-limited kinetics, is detected between 255 and 285 K.

(5) For 1 ML of ethylene on Ag(111), the electron-induced dissociation and desorption has an electron energy threshold of 10 eV. Above the threshold, the cross-section for dissociation and desorption increases monotonically with electron energy and is $(5.3 \pm 0.5) \times 10^{-17}$ cm^2 at 50 eV. Molecular ethylene desorption during electron irradiation is a minor channel and accounts for only 10–15% of a total electron-driven process (dissociation and desorption). Electron-induced dissociation results in almost equal amounts of vinyl fragments retained on the surface and desorbed into the gas phase during electron irradiation.

Acknowledgment. This work was supported by the U.S. Department of Energy, Office of Basic Sciences.